

Hysteretic resistance spikes in quantum Hall ferromagnets without domains

Henrique J. P. Freire and J. Carlos Egues

Departamento de Física e Informática, Instituto de Física de São Carlos,
Universidade de São Paulo, 13560-970 São Carlos, São Paulo, Brazil

(Dated: December 17, 2004)

We use spin-density-functional theory to study recently reported hysteretic magnetoresistance ρ_{xx} spikes in Mn-based 2D electron gases [Jaroszyński *et al.* Phys. Rev. Lett. **89**, 266802 (2002)]. We find hysteresis loops in our calculated Landau fan diagrams and total energies signaling quantum-Hall-ferromagnet phase transitions. Spin-dependent exchange-correlation effects are crucial to stabilize the relevant magnetic phases arising from *distinct* symmetry-broken excited- and ground-state solutions of the Kohn-Sham equations. Besides hysteretic spikes in ρ_{xx} , we predict *hysteretic dips* in the Hall resistance ρ_{xy} . Our theory, *without* domain walls, satisfactorily explains the recent data.

PACS numbers: 73.43.-f, 75.10.Lp, 71.15.Mb, 75.50.Pp

Two-dimensional electron gases (2DEGs) under strong magnetic fields exhibit fascinating physical phenomena; the mostly widely known of these being the integer and fractional quantum Hall effects [1]. Spontaneous magnetic order in quantum-Hall systems is yet another interesting possibility. Quantum Hall ferromagnetism arises from the interplay of the Zeeman, Coulomb, and thermal energies within the macroscopically degenerate Landau levels of the 2DEG [2, 3]. Landau level crossings [4] offer a convenient means to probe symmetry-broken quantum-Hall ferromagnetic transitions. At crossings, opposite-spin levels can benefit from Coulomb exchange to form spin-ordered states at low temperatures [2].

Many groups have investigated quantum Hall ferromagnetism in the integer and fractional quantum-Hall regimes by inducing Landau level crossings via tilted magnetic fields, density and level tuning via gate electrodes, hydrostatic pressure [5], and the *s-d* exchange-induced level bowing in Mn-based 2DEGs [6, 7]. These studies [5, 6, 7] find ubiquitous “anomalous” peaks and hysteretic spikes in Shubnikov-de-Haas measurements of the magnetoresistance ρ_{xx} . The hysteretic behavior here means that the spikes appear at distinct magnetic fields as the field is swept up and down. In the fractional quantum-Hall regime recent experiments show that these features follow from the hyperfine coupling between electrons and nuclei [8]. In the integer quantum Hall regime, the hysteretic spikes have been suggested to arise from charge transport along long domain-wall loops acting as one-dimensional (“percolating”) channels in the 2DEG near an Ising-like quantum-Hall ferromagnet transition [9]. Though appealing, this description is largely qualitative: no magnetotransport quantities (e.g., ρ_{xx}) have been calculated so far accounting for domain walls.

Alternate picture for the hysteretic spikes. In this Letter we apply the Spin Density Functional Theory (SDFT) [10] implemented via the Kohn-Sham (KS) scheme in a Local Spin Density Approximation (LSDA) to determine the electronic structure of a 2DEG, which we then use in a linear response model [11] to explicitly calculate ρ_{xx}

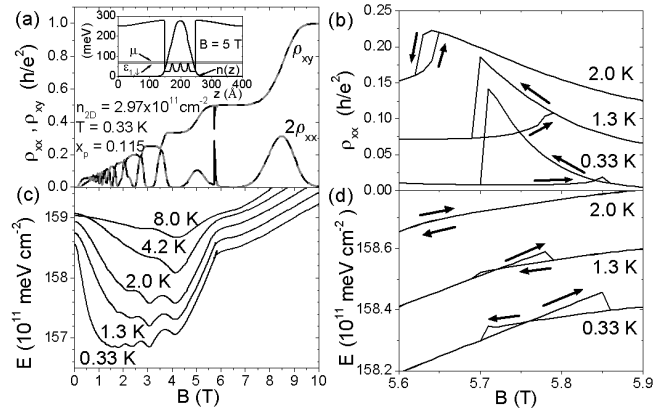


FIG. 1: Hysteretic magnetoresistance ρ_{xx} , Hall resistance ρ_{xy} , and total energy E , as a function of B for a quantum well [inset in (a)]. For the up-down B sweeps, hysteretic spikes and dips appear in ρ_{xx} and ρ_{xy} , respectively, at $B \sim 5.8$ T (a). For increasing temperatures the hysteretic loops become less pronounced (ρ_{xy} not shown) and disappear above a critical temperature $T_c \sim 2.1$ K (b). The total energy E (c) shows hysteretic loops [see blow-up of the loops in (d)] because the KS equations have two distinct solutions (ground and excited states), e.g., for $B_c^d < B < B_c^u$. These are quantum-Hall ferromagnet phases with distinct spin polarizations (Fig. 2). The curves in (b) are displaced vertically for clarity.

and ρ_{xy} . For concreteness, we focus on the experiment of Jaroszyński *et al.* [7] in Mn-based 2DEGs [12]. Interestingly, we find hysteretic behavior in ρ_{xx} and ρ_{xy} , Figs. 1(a)-(b), *without* taking into account domain walls. This behavior follows from our system having two self-consistent KS solutions – for a *same* set of parameters – with distinct total energies as shown in Figs. 1(c)-(d), see e.g. range $B_c^d < B < B_c^u$. As we discuss later on, these solutions correspond to ground and excited states describing distinct quantum Hall ferromagnetic phases of our interacting 2DEG, and, most importantly, provide a concrete example for a theorem of Perdew and Levy on the existence of excited states from ground-state density

functionals [13]. These phases comprise differing sets of conducting states contributing to the magnetotransport and hence have distinctive ρ_{xx} 's and ρ_{xy} 's. The hysteresis then arises because the 2DEG can go through a different sequence of magnetic phases (i.e., the system can become trapped into distinct local minima) as the B field is swept up and then down, e.g., phases I to II in the up sweep at $B \simeq B_c^u$ and phases III to IV in the down sweep at $B \simeq B_c^d \neq B_c^u$, Fig. 1(d). We predict *hysteretic dips* (and peaks [12]) in ρ_{xy} [14] [Fig. 1(a)] and that the spikes shift to opposite directions (Fig. 3) in samples with positive and negative g factors, for increasing tilt angles of B .

Mn-based system. We consider a CdTe quantum well between $\text{Cd}_{0.8}\text{Mg}_{0.2}\text{Te}$ barriers, with three evenly spaced $\text{Cd}_{1-x_p}\text{Mn}_{x_p}\text{Te}$ monolayers (“Mn barriers”) in the well region [7], Fig. 1(a) (inset); x_p is the planar concentration of Mn. Adjacent to the barriers lie two symmetric n-doped regions [15]. In an external field B , the *s-d* exchange interaction between the electrons in the well (2DEG) and those of the localized *d* orbitals of the Mn gives rise to a spin-dependent electron potential

$$v_{s-d}^{\sigma_z}(z; B, T) = \frac{\sigma_z}{2} N_0 \alpha \bar{x}(z) \frac{5}{2} B_{5/2} \left[\frac{5\mu_B B}{k_B(T+T_0)} \right], \quad (1)$$

where $N_0\alpha$ is the *s-d* exchange constant, $B_{5/2}$ is the spin-5/2 Brillouin function, $\bar{x}(z)$ and T_0 are the effective Mn profile and temperature [16], respectively, and $\sigma_z = \pm 1$ (or \uparrow, \downarrow) denotes the electron spin components. The structural confining potential of the well is assumed square $v_w(z) = v_0[\Theta(-L/2-z) + \Theta(L/2+z)]$ with depth v_0 ; $\Theta(z)$ is the Heaviside function. The structural potential of the Mn barriers is $v_b(z) = v_1 x(z)$; v_1 is the barrier height and $x(z)$ the nominal gaussian Mn profile.

Kohn-Sham approach. We use the SDFT [10] formulated in the context of the effective-mass approximation of semiconductors. Within the finite-temperature formulation of Mermin [17, 18], we obtain the KS equations

$$\left[-\frac{\hbar^2}{2m} \frac{d}{dz^2} + v_{\text{eff}}^{\sigma_z}(z; [n_{\uparrow}, n_{\downarrow}]) \right] \chi_i^{\sigma_z}(z) = \varepsilon_i^{\sigma_z} \chi_i^{\sigma_z}(z), \quad (2)$$

where m is the effective mass, $i = 1, 2 \dots$ the band index, and $v_{\text{eff}}^{\sigma_z}(z; [n_{\uparrow}, n_{\downarrow}])$ the effective single-particle potential

$$v_{\text{eff}}^{\sigma_z}(z; [n_{\uparrow}, n_{\downarrow}]) = v_s(z) + v_{s-d}^{\sigma_z}(z) + v_h(z; [n]) + v_{xc}^{\sigma_z}(z; [n_{\uparrow}, n_{\downarrow}]). \quad (3)$$

In Eq. (3) $v_s(z) = v_w(z) + v_b(z)$, $v_h(z; [n])$ is the Hartree potential, calculated by solving Poisson's equation, and $v_{xc}^{\sigma_z}(z; [n_{\uparrow}, n_{\downarrow}])$ is the *spin-dependent* exchange-correlation (XC) potential [19]. The motion in the xy plane is quantized into Landau levels with energies $\varepsilon_n = (n + 1/2)\hbar\omega_c$, $n = 0, 1, 2, \dots$ and $\omega_c = eB/m$ [20]. The total wavefunction is $\psi_{i,n,k_y}^{\sigma_z}(x, y, z) = \frac{1}{\sqrt{L_y}} \exp(i k_y y) \varphi_n(x) \chi_i^{\sigma_z}(z)$, where $\varphi_n(x)$ is the n -th

harmonic oscillator eigenfunction centered at $x_0 = -\hbar k_y/m\omega_c$ and k_y is the electron wave number along the y axis; L_y is a normalizing length. This decoupling of the z and xy motions follows from the uniformness of the total electron density within the xy plane: because each electron can be anywhere within the plane, we use the average total electron density $n(z) = \sum_{i,n,k_y,\sigma_z} f_{i,n}^{\sigma_z} \frac{1}{L_x L_y} \int \int |\psi_{i,n,k_y}^{\sigma_z}|^2 dx dy = \sum_{i,n,k_y,\sigma_z} |\chi_i^{\sigma_z}(z)|^2 f_{i,n}^{\sigma_z}$ in Poisson's equation, instead of $n(x, y, z)$ [here $f_{i,n}^{\sigma_z}$ is the Fermi function and L_x is a normalizing length]. This procedure makes the 2DEG uniform thus rendering a separable KS set.

We assume that the KS eigenvalues

$$\varepsilon_{i,n}^{\sigma_z} = \varepsilon_i^{\sigma_z}(B) + \left(n + \frac{1}{2} \right) \hbar\omega_c + \frac{\sigma_z}{2} g\mu_B B, \quad (4)$$

where $g\mu_B B \sigma_z/2$ is the ordinary Zeeman term (g : effective Landé factor), describe the actual electronic structure of our 2DEG. This assumption is, in principle, unjustified within DFT: the individual KS orbitals represent states of a fictitious non-interacting electron gas in an effective potential, Eqs. (2) and (3). With this assumption, however, we satisfactorily explain observed hysteretic phenomena in 2DEGs [7, 12].

System parameters. In our simulations we use (see Ref. [7]): $m/m_0 = 0.099$, dielectric constant $\epsilon/\epsilon_0 = 10$, $g = -1.67$, $N_0\alpha = 220$ meV, quantum-well width $L = 100$ Å, spacer width $L_s = 200$ Å, $n_{2D} = 2.97 \times 10^{11}$ cm $^{-2}$, number of Mn monolayers $N_b = 3$, $x_p = 0.115$, $v_0 = 248.1$ meV, $v_1 = 1183.5$ meV, $T_0 = 0.47$ K, and assume a diffusion length $\ell \sim 4.67$ Å for the Mn profile.

Figures 1 and 2 show our theoretical results for ρ_{xx} , ρ_{xy} 1(a)-(b), total energy E 1(c)-(d), Landau level fan diagram 2(a), spin-resolved electron densities $n_{2D}^{\uparrow, \downarrow}$ 2(b), and spin-polarization ζ 2(c). Remarkably, all of these quantities show abrupt hysteretic changes near 5.8 T as the B field is swept up and down. The discontinuous nature of these features follows from the 2DEG undergoing (quantum) phase transitions in which its degree of spin polarization ζ suddenly changes, 2(b)-(c), e.g., in the down sweep the 2DEG becomes highly spin-polarized near 5.8 T [2(c)]: a quantum Hall ferromagnetic phase transition takes place. Our calculated fan diagram 2(a) and total energy 1(d) corroborate this scenario: the opposite-spin levels $\varepsilon_{1,0}^{\uparrow}$, $\varepsilon_{1,1}^{\downarrow}$ suddenly cross near μ thus lowering the total energy E [see III to IV discontinuity in 1(d)]. This is similar to the Giuliani-Quinn instability where the 1st-order transition is due to the gain of exchange energy in the ferromagnetic state [2]. Our calculation also includes *correlation* which somewhat reduces the exchange effects. The role of the *s-d* exchange [Eq. (1)] in our system is to cause “level bowing” ($B < 2$ T) thus inducing opposite-spin Landau level crossings, see e.g. crossings for $B < 4$ T in 2(a). When crossings occur near μ , spin-dependent XC effects may induce phase transi-

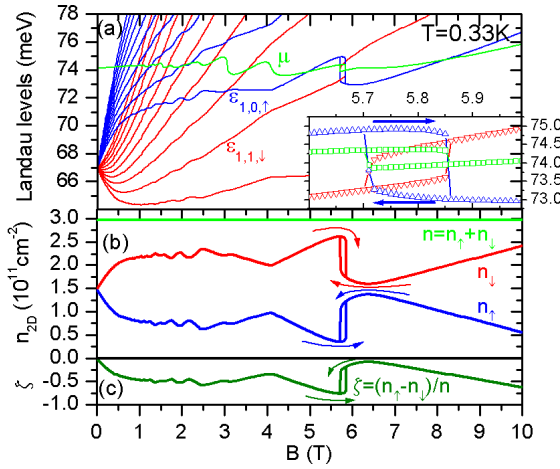


FIG. 2: Landau-level fan diagram [Eq. 4] (a), spin-dependent electron densities $n_{2D}^{\uparrow, \downarrow}$ (b), and spin polarization ζ (c) of our 2DEG [Fig. 1(a)]. In (a) we plot the center of each Landau level with a phenomenological gaussian broadening $\Gamma = 0.36\sqrt{B}$ meV T $^{-1/2}$ [11]. The s - d induced non-linear behavior of the energy spectrum ($B < 2$ T) allows for non-trivial Landau level crossings near the chemical potential μ (curve at ~ 74 meV). Inset (a): blow-up of the hysteretic crossings between the states with $n = 1$ and spin down ($\varepsilon_{1,1}^{\downarrow}$) and that with $n = 0$ and spin up ($\varepsilon_{1,0}^{\uparrow}$) at $B \sim 5.8$ T for the up=down B sweeps. The discontinuous change in the spin-polarization ζ signals a transition between distinct quantum-Hall ferromagnet phases. We have adjusted x_p and Γ so the levels would cross at ~ 5.8 T as in the experimental data [7].

tions (e.g. at 5.8 T); we do not find phase transitions in a Hartree calculation. The phases here are those of an Ising-like itinerant 2D ferromagnet with Pauli magnetization $(n_{\uparrow} - n_{\downarrow})\mu_B = n_{2D}\zeta\mu_B$. Next we show how hysteresis arises in our SDFT calculation.

Excited and ground Kohn-Sham states. Using the constrained-search definition of the ground state functional $E_v[n]$ (defined on domain of densities constructed from any wave function), Perdew and Levy [13] have shown that “...every extremum of $E_v[n]$ represents the density $n_i(\mathbf{r})$ and the energy E_i of a stationary state. The absolute minima represent the ground states, and the extrema lying above the minimum represent a subset of the excited states.” These authors have also proved that some of the self-consistent solutions of the KS equations extremize $E_v[n]$, provided that these solutions obey ground-state Fermi statistics (*aufbau* principle) with a *single* chemical potential – this is a necessary and sufficient condition. These theorems have been generalized to SDFT [21] and hence hold in our system.

Our simulations show that for a certain window of magnetic field [e.g., $B_c^d < B < B_c^u$ in Fig. 1(d)] the KS equations (2) have indeed two self-consistent solutions [22] with distinct total energies and spin polarizations [18] – both satisfying the necessary and sufficient

condition above. At each B in this range, one of these two solutions is stable (true minimum, ground state) and the other metastable (local minimum, excited state). In practice, these two states (phases) are separated by an energy barrier [23] which may trap the system in the metastable states during the up=down B sweeps thus giving rise to hysteretic loops, Figs. 1 and 2.

Magneto-transport. We obtain the longitudinal and Hall resistances from the conductivity tensor ($\rho = \sigma^{-1}$), calculated within the self-consistent Born-approximation model of Ando and Uemura [11]. For short-range scatterers, $\sigma_{xx} = \frac{4e^2}{h} \int_{-\infty}^{\infty} \left(-\frac{\partial f(\varepsilon)}{\partial \varepsilon} \right) \sum_{i,n,\sigma_z} (n + \frac{1}{2}) \exp \left[-\left(\frac{\varepsilon - \varepsilon_{i,n}^{\sigma_z}}{\Gamma_{\text{ext}}} \right)^2 \right] d\varepsilon$ and $\sigma_{xy} = en_{2D}/B + \Delta\sigma_{xy}$; $\Delta\sigma_{xy}$ is a small correction [11]. We model the extended Landau states by a gaussian $g_{\text{ext}}(\varepsilon)$ of width $\Gamma_{\text{ext}} = 0.25$ meV [24].

Hysteretic resistance spikes and dips. The ordinary ρ_{xx} peaks in Fig. 1(a), e.g., at 2.5, 3.1, and 5 T, are due to subsequent *single* Landau levels crossing the chemical potential μ and appear between plateaus in ρ_{xy} . Though involving the crossing of *two* opposite-spin levels at μ , the ρ_{xx} spike at $B \sim 5.8$ T has the same physical origin as the ordinary peaks: electrons in partially filled crossing levels are susceptible to scattering (“dissipation”) which increases ρ_{xx} . This spike, however, corresponds to a dip in a plateau of ρ_{xy} : as the two Landau levels cross near μ , the number of conducting channels n_c “fluctuates” thus making ρ_{xy} dip ($\Delta n_c > 0$) [or peak ($\Delta n_c < 0$)] toward an adjacent plateau consistent with n_c . Whether ρ_{xy} dips or peaks and whether the spikes and dips are stronger in the up or down sweeps depend on the details of the crossings at μ , Fig. 2(a) – these features are, however, hysteretic as n_c differs in the up and down B sweeps. For increasing tilt angles θ , Fig. 3, the hysteretic spike shifts to lower fields while the ordinary Shubnikov-de-Haas maxima do not. Figure 3 uniquely identifies ordinary (single Landau levels crossing μ) and “anomalous peaks” (two Landau levels crossing μ) in ρ_{xx} .

Hysteresis & critical temperature. Figure 4(a) shows

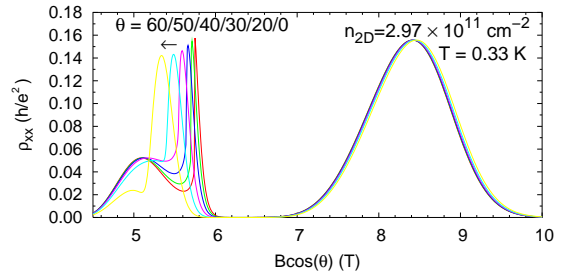


FIG. 3: Magneto-resistance ρ_{xx} vs $B \cos(\theta)$ for several tilt angles θ between the B field and the growth direction. Similarly to the data in [7], the spike shifts to lower fields as θ increases, while the ordinary Shubnikov-de-Haas peaks do not.

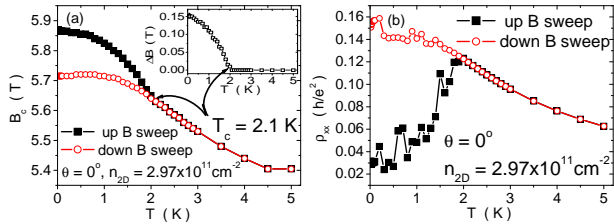


FIG. 4: Temperature dependence of the ρ_{xx} spike positions B_c (a) and amplitudes (b) for up \rightleftharpoons down B sweeps. Inset in (a): $\Delta B_c = B_c^u - B_c^d$ versus T from which we extract a critical temperature T_c ; for $T > T_c$ the hysteresis disappears. The asymmetric shape of our hysteretic loops [Figs. 1(b)-(d)] is clearly manifest in (b).

the hysteresis in the ρ_{xx} spike position B_c as a function of T : $B_c^u > B_c^d$ for the up \rightleftharpoons down B sweeps. By plotting $\Delta B_c = B_c^u - B_c^d$ versus T we can extract a critical temperature T_c above which $\Delta B_c = 0$. We find [inset in 4(a)] $T_c = 2.1$ K which is comparable to the experimental value 1.3 K [7]. The *amplitude* of the spike is also hysteretic, Fig. 4(b). Here, however, only the up-sweep behavior agrees with the data [7, 15].

Further comparison with experiments. We also reproduce the *non-hysteretic* ρ_{xx} peak at ~ 3.2 T (single level crossing μ) seen in [6]. We find that the peak at ~ 2.8 T [6] arises from *two* levels crossing μ and predict that it shifts *upward* (as opposed to Fig. 3 here) as θ increases because $g > 0$ in [6] while $g < 0$ in [7]. However, we do not find any hysteretic behavior here. Essentially, the non-integer filling factors near the opposite-spin level crossings in [6] (as opposed to [7]) result in exchange energy gains not enough to induce phase transitions.

Final remarks. (i) Quenched-disorder-induced domains – not domains arising in metastable states [9, 25] – can lead to transport anisotropies in 2DEGs [26, 27]. (ii) The relevance of the hyperfine coupling to the hysteretic phenomena has been recognized experimentally only in the *fractional* quantum Hall regime. We account for disorder effects only via the broadening of the Landau levels and neglect the hyperfine coupling and domains altogether. Our successful description of hysteretic (quantum Hall) ferromagnetic phenomena in 2DEGs highlights the power of DFT in a non-conventional application.

We thank R. Knobel, N. Samarth, and J. Jaroszyński for providing details of the experiments and K. Capelle for helpful discussions. JCE acknowledges enlightening discussions with J. P. Perdew, O. Gunnarsson, M. Governale, M. R. Geller, M. E. Flatté and L. J. Sham. This work was supported by FAPESP and CNPq.

- [1] *Perpectives on Quantum Hall effects*, edited by S. Das Sarma and A. Pinczuk (Wiley, New York, 1997).
- [2] G. F. Giuliani and J. J. Quinn, Phys. Rev. B **31**, 6228 (1985); S. M. Girvin and A. H. MacDonald in Ref. 1.
- [3] Disorder effects can be important near $\nu = 1$; see J. Sinova *et al.*, Phys. Rev. B **62**, 13579 (2000).
- [4] F. F. Fang and P. J. Stiles, Phys. Rev. **174**, 823 (1968).
- [5] T. Jungwirth *et al.* Phys. Rev. Lett. **81**, 2328 (1998); H. Cho *et al.* *ibid.* **81**, 2522 (1998); V. Piazza *et al.*, Nature **402**, 638 (1999); J. Eom *et al.*, Science **289**, 2320 (2000); E. P. De Poortere *et al.*, *ibid.* **290**, 1546 (2000); J.H. Smet *et al.*, Phys. Rev. Lett. **86**, 2412 (2001); M. Chen *et al.*, *ibid.* **91**, 116804 (2003); G. M. Gusev *et al.* Phys. Rev. B **67**, 155313 (2003).
- [6] R. Knobel *et al.*, Phys. Rev. B **65** 235327 (2002).
- [7] J. Jaroszyński *et al.*, Phys. Rev. Lett. **89**, 266802 (2002).
- [8] J. H. Smet *et al.*, Nature **415**, 281 (2002); O. Stern *et al.*, Phys. Rev. B **70** 075318 (2004).
- [9] T. Jungwirth and A. H. MacDonald, Phys. Rev. Lett. **87**, 216801 (2001).
- [10] W. Kohn and P. Vashishta, in *Theory of Inhomogeneous Electron Gas*, edited by S. Lundqvist and N. H. March (Plenum, New York, 1983).
- [11] T. Ando and Y. Uemura, J. Phys. Soc. Jpn **36**, 959 (1974); R. R. Gerhardt, Surf. Sci. **58**, 227 (1976).
- [12] We find hysteretic phenomena also in the non-magnetic systems of [5] in the integer quantum Hall regime.
- [13] J. P. Perdew and M. Levy, Phys. Rev. B **31**, 6264 (1985).
- [14] A weak dip in ρ_{xy} appears in Ref. [7] (J. Jaroszyński, private communication). Our calculated dips are more pronounced. Further work is needed to address this point.
- [15] The sample in Ref. [7] is doped on one side only.
- [16] J. K. Furdyna, J. Appl. Phys. **64**, R29 (1988).
- [17] N. D. Mermin, Phys. Rev. **137**, A1441 (1965).
- [18] O. Gunnarsson and B. I. Lundqvist, Phys. Rev. B **13**, 4274 (1976).
- [19] S. H. Vosko *et al.*, Can. J. Phys. **58**, 1200 (1980). Other XC parameterizations yield qualitatively similar results.
- [20] Landau quantization is properly accounted for in the KS equations of the rigorous current-spin-density-functional theory of Vignale and Rasolt; see Eq. (8) in Phys. Rev. Lett. **59**, 2360 (1987). Our approach is equivalent to neglecting both (i) the paramagnetic current density (in the XC functional E_{XC}) and (ii) the XC vector potential A_{XC} in their Eq. (8).
- [21] J. P. Perdew, unpublished.
- [22] We solve the self-consistent equations for subsequent B fields by using the solution at a particular B as the input configuration to find the solution with the field slightly (i) increased $B + \Delta B$ in the upsweep or (ii) decreased $B - \Delta B$ in the downsweep. We note that two distinct solutions arise only when $v_{xc}^{\sigma z} \neq 0$.
- [23] The nature of this barrier and its collapse as the metastable state disappears needs further investigation. However, its existence does not require domain walls (e.g. Stoner-Wohlfarth theory of hysteresis).
- [24] Our $g_{ext}(\varepsilon)$ is normalized as if *all* electrons were extended (conducting). This is justified because the loss of Hall current by the formation of localized states is exactly compensated by the remaining extended electrons [see, R. E. Prange, Phys. Rev. B **23**, R4802 (1981)].
- [25] L. Brey and C. Tejedor, Phys. Rev. B **66**, 041308(R) (2002).
- [26] J. T. Chalker *et al.*, Phys. Rev. B **66**, 161317 (2002).
- [27] Note, however, that U. Zeitler *et al.* [Phys. Rev. Lett. **86**, 866 (2001)] explain their data via the formation of a unidirectional stripe phase in the plane of the 2DEG. See also: W. Pan *et al.*, Phys. Rev. B **64**, 121305(R) (2001).

